'95 KACC (1995. 10. 23 ~ 25)

ACOUSTIC EMISSION IN BENDING FATIGUE PROCESS OF CARBURIZING SPUR GEAR BY AE SOURCE LOCATION

°Hirofumi SENTOKU* and Hiroyuki YAMATO*

*Dep. of Mechanical Engineering , Yamaguchi University , 2557 Tokiwadai , Ube , 755, Japan
Tel:81-0836-35-9918;Fax:81-0836-35-9926

Abstract It is important from prevention of the malfunction and an important accident by the failuer, to detect a failuer in revolution devices. The acoustic emission(AE) method is expected as means that defects an abnormal phenomenon of revolution devices earlily and utilized. Although a research example by the AE method is reported regarding a gears, little reserch has been conducted using the AE method for running gears in a bending fatigue process of spur gear teeth. Therefore, in this report , with two micro AE sensors attached to the side of the gear, AE was measured in a bending fatigue process of a carburizing gear by using the power circurating-type machine and AE source location in gear teeth were required. By various analysis in these data, the AE characteristics in the fatigue damaging process of the gear tooth were determined.

Keywords Gear, Acoustic Emission, AE Source Location, Crack Length

1. INTRODUCTION

It is important in the prevention of malfunctions and accidents , to detect failure in revolution devices. As a means of detecting abnormalities in revolution devices at an early stage, AE method has been effectively applied[1]. Research examples[2], [3] concerning gears included in revolution devices by using AE method have been reported . However, almost no research using the AE methods has been conducted with regard to running gears in a bending fatigue process of spur gear teeth. Therefore, in the previous report, by using a power circulating-type gear testing machine, AE signals and crack length were measured in the bending fatigue process of a carburizing gear with AE sensor on the gear box. Furthermore, the envelope of the AE signal was detected and the AE signal were recorded in the data recorder . Afterwards, they were added synchronously , averaged and analyzed. However, it is necessary to detect abnormalities of running gear in real time. Terefore, in this paper, spur gears with two micro AE sensors on one side of a gear were rotated by using a power-circulating type gear testing machine. AE by gears and by bearings were separated by two micro AE sensors. In bending fatigue process , the location of gear tooth cracked were decided and it was examined to detect the advance of crack in real time.

2. TEST GEARS AND METHOD OF EXPERIMENT

2.1 Test Gears

The test gears were carburizing steel SNC815 . The hardness of the carburizing gear was 595 Hv on the surface and 390 Hv in the interior. The dimensions are shown in Table 1.

Table 1 Dimension of test gears

		Pinion	Gear
Module	m	4 mm	
Pressure angle	α_0	20°	
Number of teeth	z	27	31
Addendum modification coefficient	x	-0.1	0
Facewidth	b	10mm	
Method of finishing teeth		Hobbed	
Accuracy		4 grade	
Material		SNC815	
Heat treatment		Carburized & quenched	

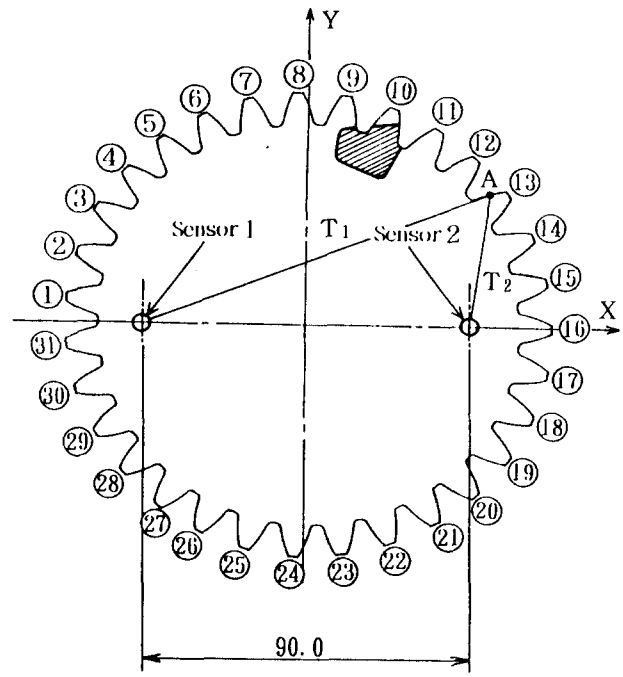

Fig. 1 Tooth numbers of test gear and positions of two sensors

2.2 Method of Experiment

The power circulating-type gear testing machine was used. The number of revolution of the pinion and gear shaft were 442 and 385 rpm respectively. About 0.5 ℓ /min oil was poured on the tooth flank. Gears were loaded by a coupling to give torque. The normal forces on the tooth flank Pn of the carburizing gear were 15.1 kN . The synchronizing signal was measured by mean of a photograph transister. To cause a crack in a specific tooth, 2 mm was shaved from both sides of the fillet of the target tooth. By attaching a strain gauge of length 0.2 mm at the critical section of the tooth, the fillet stress of the tensile flank was measured. In order to measure the root stress profile in the bending fatigue process, a strain gauge was attached to the side of the tooth at the fillet on the compressive flank. To measure the crack length, the crack gauge was attached on the side of the tooth at the fillet of the tensile flank. To decide the location of gear tooth cracked and separate AE by bearings , two micro AE sensors of 3 mm diameter and thickness were screwed on one

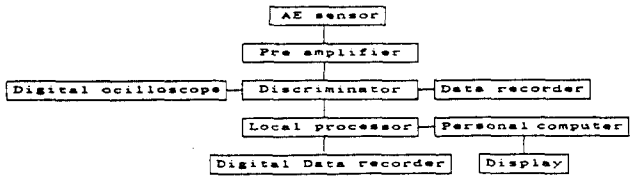

Fig.2 Block diagram for AE measurement

side gear as shown in Figure 1. The resonance frequency are about 350 kHz. Figure 2 shows the block diagram for AE measurement. The AE signal was amplified to 40 dB with a small pre-amplifier, passed through a mercury slip ring and amplified a further 50 dB with a discriminator and a local processor. The signal was band passed from 200kHz to 1000kHz and the AE signal envelope was detected. The signal was recorded in the data recorder and analyzed.

3. EXPERIMENTAL RESULTS AND CONSIDERATIONS

3.1 AE Source Location of Each Tooth

AE Source Location can be requested by a difference of such time when AE wave by one signal resource reaches a plural AE sensors. Now, point A in Figuer 1 is regarded as the location of a signal resource of AE. The arrival time of AE wave from point A to sensor 1, 2 is made T1, T2 respectively. Then, an arrival time interval becomes $\Delta T=T1-T2$. Furthermore, as shown in the next equation , ΔL difference of the distance from point A to each sensor is required by applying acoustic velocity V to this ΔT.

$$\Delta L=\Delta T\times V=(T1-T2) \qquad \cdots\cdots(1)$$

A location of each tooth can be decided by this ΔL. The distances from the tip of each tooth in Figuer 1 to two sensors were required geometrically. The difference between these two distances is made ΔL and a location of each tooth are indicated in Figuer 3. Numbers in this figure are equivalent to each tooth number in Figuer 1. Tooth 17～31 are symmetric with respect to the X-axis that passes two sensors as seen from Figure 1. Therefore, they were omitted. Next, to confirm an appropriateness of this AE source location , artificial AE signal was produced on the tip of each tooth in Figuer 1. And, this AE source location is required by obtainning time that an envelope detection signal of AE exceeds a threshold voltage and applying acoustic velocity V to the difference between their time in each sensor. Figure 4 shows the results of AE source location in tooth 1, 7and 13. The vertical axis in Figure 4 indicates AE event count, and the horizontal axis ΔL which was mentioned above. As seen from these figures, AE concentrates in particular ΔL for each tooth. And, these locations change for each tooth. And, these locations in ΔL agree well with theoretical values of each tooth in Figure 3. It was the same as for other teeth. Thermore, as making the threshold voltage higher than that mentioned above, AE source location were required. As shown in Figure 5, ΔL of tooth 7 is similar to that in Figure 4, but ΔL of tooth 1 , 13 move left and right direction respectively. This is conceivable in the following manner. Figure 6 shows artifical AE waves from tooth 1 by sensor 1, 2 . As shown in Figure 6 AE wave by sensor 1 stands sharply , because tooth 1 is near sensor 1 as seen in Figure 1. However, as tooth 1 is far from sensor 2 and it has a damping effect, rising of AE wave in sensor 2 is gentle, as seen in Figure 6. Therefore, as the threshold voltage becomes high , time difference between AE waves by two sensors increases and ΔL of tooth 1 moves for left direction as seen in Figure 5. ΔL of teeth which are located in an about equal distance from two sensors are not hardly influenced by the threshold voltage and are similar to these in Figure 3. But, as teeth are nearer one sensor , this influence becomes bigger.

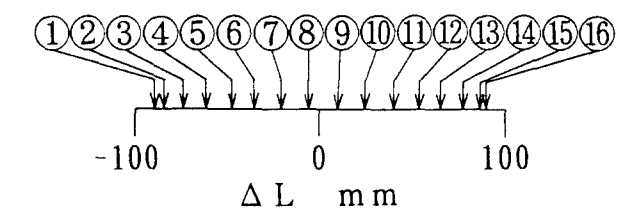

Fig.3 Calculated locations of each tooth

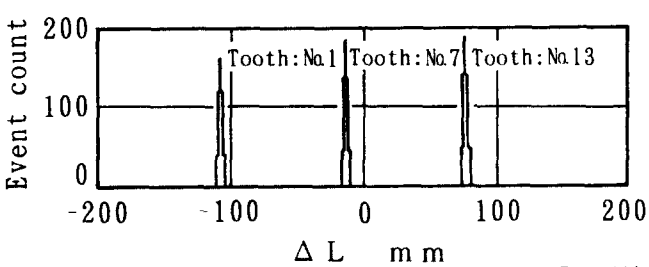

Fig.4 Measured AE source location in tooth 1, 7 and13

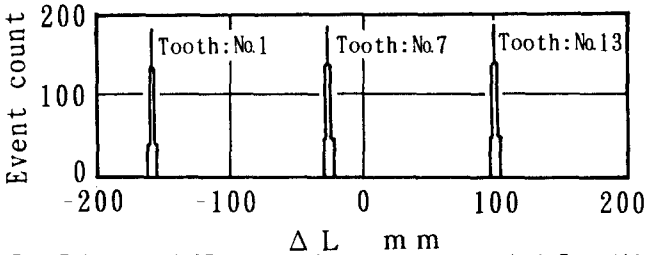

Fig.5 Measured AE source location in tooth 1, 7 and13 (In the case of higher threshold of AE signal)

3.2 AE Source Location of Bearings

In the case that a bearing is damaged in running, AE by it coexists. Thereupon, artificial AE signal was produced on the bearings that support a driven gear of test gear side. And, by using the method mentioned above , AE source location in this case was required by two sensors on the driven gear. The result is shown in Figure 7. As seen from this figure, AE by bearings appears in the neighborhood of $\Delta L=0$. It is according to that locations of bearings are

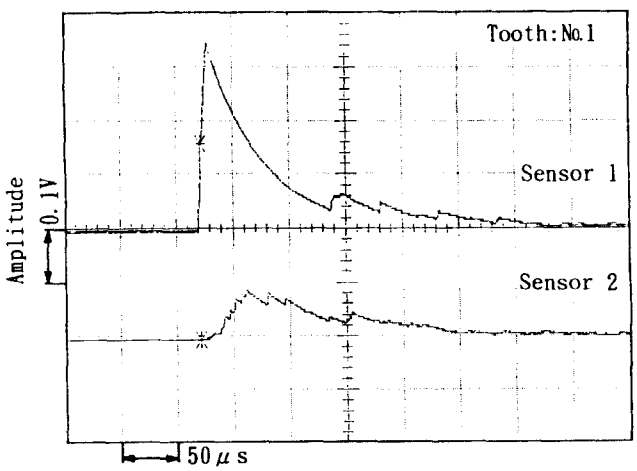

Fig.6 AE signals by each sensor

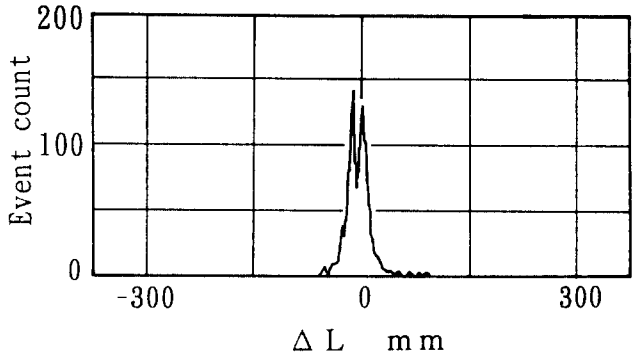

Fig.7 AE source location of bearings

in an about equal distance from two sensors. Therefore, there is an influence of bearing in the range of ΔL in Figure 8. AE in a range other than it is the one by a gear.

3.3 Crack Length and AE Source Location

First of all, AE source location was required near the specific tooth as follows. Figure 8 shows root stress profile of the specific tooth and AE signal envelope by sensor 1 simultaneously. As shown in Figure 8, there are mainely three peaks A, B and C in a range of root stress profile. Peaks A, B are caused as moving from double tooth contact to single tooth contact and peak B from single tooth contact to double tooth contact. Therefore, it is conceivable that each peak is caused by the tip corner contact. Figure 9 (a), (b) show the situation that tooth 9, 10 and 11 in the driven gear mesh. Revolution direction is the direction of the arrow. Figure 9(a) shows the condition that tooth 10 and 11 mesh simultaneously and tooth 11 meshs with the tip corner of the drive gear. It is conceivable that peak A mentioned above was caused by this tip corner contact. Also, Figure 9 (b) shows that gears revolve more a little from the case of Figure 9 (a) and tooth 10 and the tip corner of tooth 9 meshs simultaneously. Peak B is considered to be caused by the tip corner contact of tooth 9. Peak C is considered to be caused by meshing with tooth 10 and the tip corner of the drive gear. Here, source location of only AE envelope detection signal inside a range of root stress profile in Figure 8 were required. This result is shown in Figure 10. The vertical axis in this figure indicate AE event count rate (c/m) and the horizontal axis ΔL of range -300～300 mm. Furthermore, the threshold

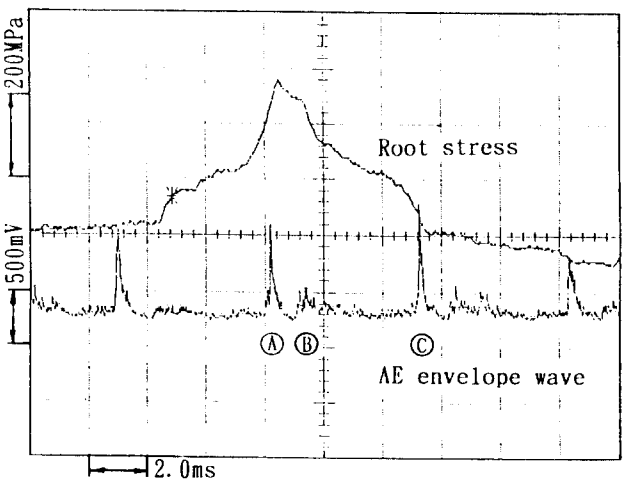

Fig.8 Root stress profile and AE envelope detection signal

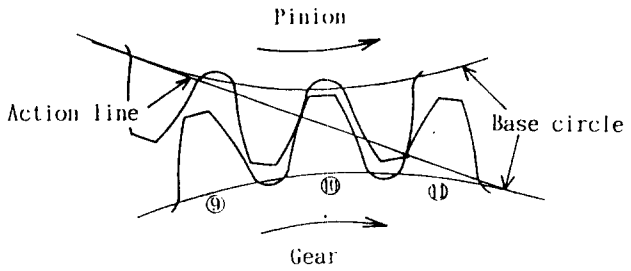

(a) Simultaneous meshing of tooth 10 and 11

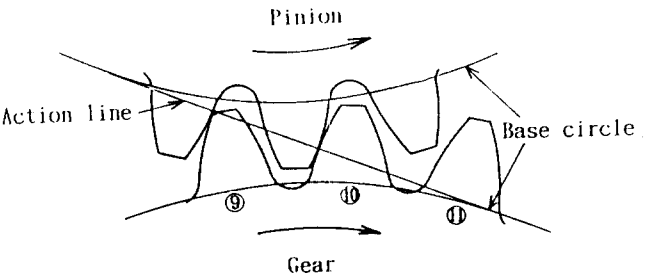

(b) Simultaneous meshing of tooth 9 and 10

Fig.9 Meshing of gears

voltage in this case is 900mV. As seen in Figure 10, the mountain having the width is seen in the neighborhood of ΔL=150 mm. This is conceivable according to that peak A, B and C were caused by tooth 9, 10 and 11 within the range of root stress profile as mentioned above. It has been confirmed that AE source location near the specific tooth was required as above. Next, these AE source location was required for number of cycles. This result is indicated in Figure 11 with crack length mesured by crack gauge[4]. The threshold voltage in this case is 900 mV as mentioned above. As seen in Figure 11, AE event count rates are distributed in similar magunitude and range to about $N=3.61\times10^4$. However, they become large in the location near ΔL=0 from about $N=3.69\times10^4$ and it becomes very large from $N=3.76\times10^4$. This very large AE is conceivable to be caused by tooth 9. This isaccording to that tooth 9 is nearest ΔL=0 within tooth 9, 10 and 11 as seen in Figure 3. To cofirm the above, the AE envelope detection signal which were added 100 times synchronously and then averaged near tooth 9 were required for each number of cycle were shown in Figure 12. As seen in Figure 12, peak B by tip corner contact of tooth 9

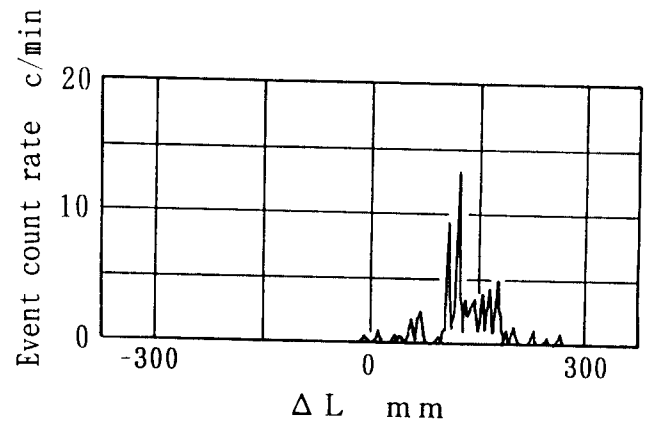

Fig.10 Source location of AE envelope detection signal within the range of root stress profile

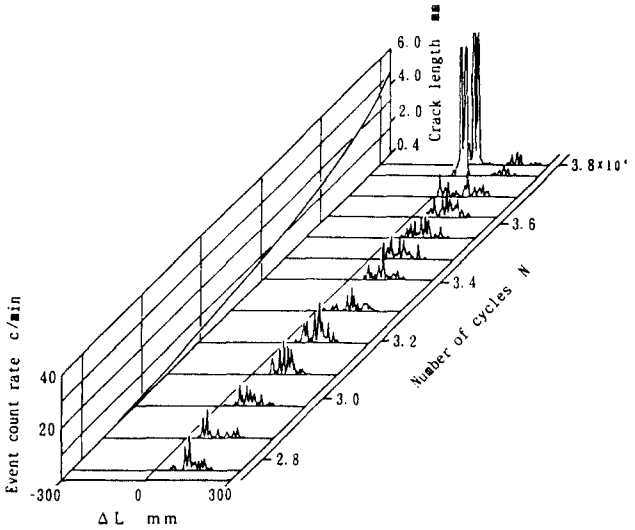

Fig. 11 AE source location and crack length

is smaller than peak A, C in $N=2.93\times10^4$. However, although peak A, C do not changevery much in $N=3.77\times10^4$, peak B becomes very large. Therefore, it is conceivable that peak B does not exceed hardly the threshold voltage to $N=3.62\times10^4$. Peak B begines to exceed gradually it from $N=3.69\times10^4$, and AE event count rate appeares in the location near $\Delta L=0$ as seen in Figure11. As number of cycles increase moreover, AE event count rate becomes very large in this location. The reason why AE event count rate becomes large in tooth 9 as above is conceivable as follows. As the specific tooth 10 in Figure 9 (b) is cracked and the crack becomes large, the spring stiffness of this tooth becomes small and the load assignment of the tip in tooth 9 becomes large. Therefore, it is conceivable that the tooth flank was rubbed vigorously by the tip corner contact. Furthermore, AE amplitude and AE energy were requided for ΔL. Figures 13 (a), (b) show these results. All of them become largest near $\Delta L=0$ from $N=3.69\times10^4$ in the same manner as AE event count rate. And, this tendency is remarkable in the case of AE energy.

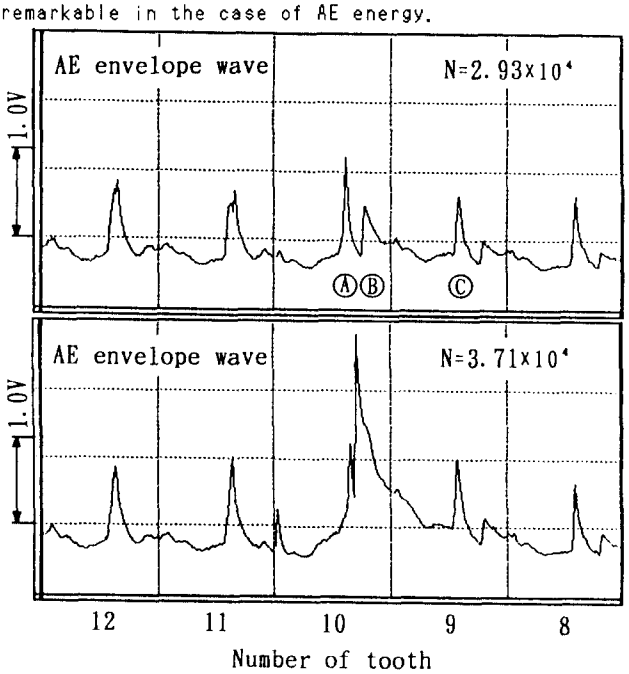

Fig. 12 Average of AE envelope detection signal

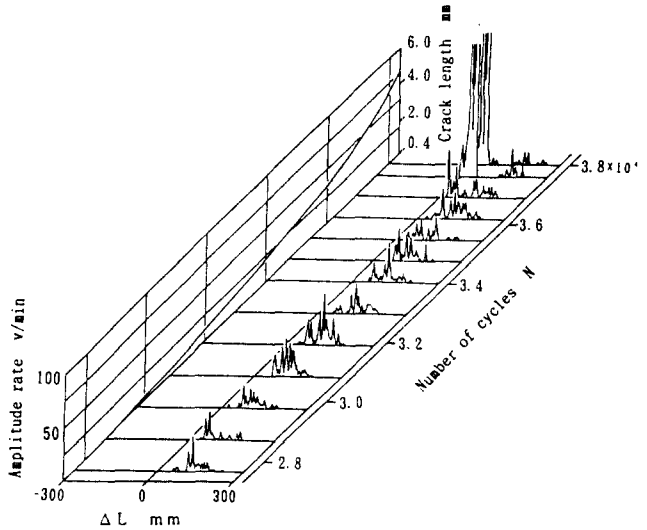

(a) AE amplitude

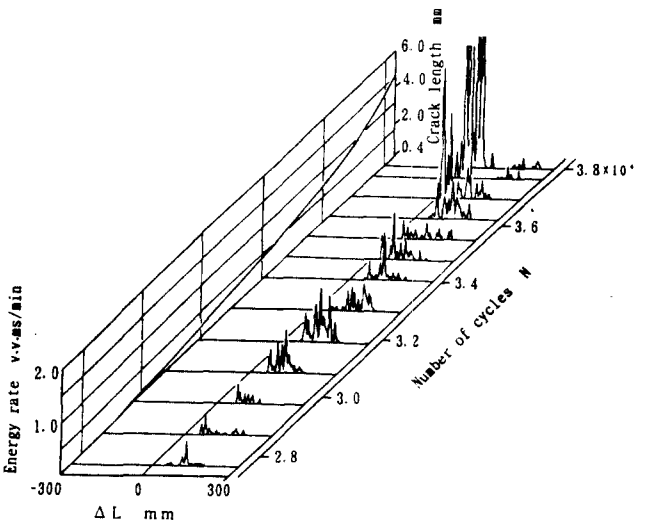

(b) AE energy

Fig. 13 AE source location and crack length

4. CONCLUSION

AE source location and crack length were measured in the bending fatigue process of carburizing gear by using a power circulating-type gear testing machine. As a result, it was concluded that;

(1) AE source locations in each gear tooth and bearings can be required by using two micro AE sensors.
(2) By measuring AE source locations of gear teeth, the advance of cracks on gear teeth can be known in real time.
(3) AE amplitude and AE energy become gradually large with increase of crack length. And, this tendency is remarkable in the case of AE energy.

REFERENCES

[1] I. Sato and 4 others, 1989 National Conference on AE, pp. 112, 1989. [2] K. Kondo and J. Takada, Symposium "Gear and Transmission Mechanism", 890-58, pp. 303, 1989. [3] S. Oda, Y. Miyachika and T. Koide, Trans. JSME, Ser C, 58-551, pp. 2219, 1992. [4] H. Sentoku and 1 other, Trans. JSME, Ser C, 61-582, pp. 417, 1995.